A Novel Approach for Reducing Dental Filling Artifact in CT-Based Attenuation Correction of PET Data

M. Abdoli[1,2], M.R. Ay[1,2†], A. Ahmadian[1,2], N. Sahba[2] and H. Zaidi[3]

[1]Tehran University of Medical Sciences, Department of Medical Physics and Biomedical Engineering, Tehran, Iran
[2]Tehran University of Medical Sciences, Research Center for Science and Technology in Medicine, Tehran, Iran
[3]Geneva University Hospital, Division of Nuclear Medicine, Geneva, Switzerland

Abstract — **Reliable attenuation correction methods in PET require accurate determination of the attenuation map (µmap), which represents the spatial distribution of linear attenuation coefficients (LACs) at 511 keV for the region under study. Since CT image pixel intensities are directly related to the LAC of the corresponding tissue calculated from the effective CT energy, the µmap at 511 keV can be directly generated from the CT images. The presence of high density dental fillings material in head and neck CT imaging is known to generate strong streak artifacts in the µmap which will likely propagate to the resulting PET images during CT-based attenuation correction (CATC). The purpose of this work is to develop a fast approach for reduction of dental filling artifacts in the generated µmap. Currently available sinogram based metal artifact reduction (MAR) algorithms are based on correction of raw data sinograms which are huge files usually stored in proprietary format not generally disclosed by manufacturers and thus are not straightforward to handle. Our method uses the concept of virtual sinograms for implementation of MAR, which are produced by forward projection of CT images in Dicom format. The projection data affected by metallic objects are detected in the sinogram space by segmentation of metallic objects in the CT image followed by forward projection of the metal-only image. Thereafter the affected projections are replaced by interpolated values from adjacent projections using the spline interpolation technique. The algorithm was applied to a dedicated phantom experiment scanned before and after metal insertion, where the corrected and non-corrected µmaps were compared to the artifact-free µmap. It was observed that by using this fast method, the mean relative error in regions close to metallic objects is ~35% without correction and decreases to ~5% after correction.**

Keywords — **PET/CT, Attenuation Correction, Metal Artifact, CTAC**

I. Introduction

One of the growing technologic advances in recent years is the application of combined PET/CT scanners which make use of two physically different techniques in order to fulfill the drawbacks of each single imaging modality. A combined PET and CT in a single device can overcome misregistration problems originating from internal organ movements, variations in scanner bed profile and positioning of the patient. Combining functional data with anatomic localization via PET/CT dual-modality image registration can dramatically improve the potential of molecular PET imaging for diagnosis, treatment planning and prognosis assessment.

In PET/CT structural and functional images are used synchronously and the CT images are used for correction of attenuation of PET data. CT imaging is usually performed using 80-140 kVp, which is fairly below the 511keV energy used in PET. Converting the range of energy by attenuation map correction is thus mandatory. The conventional approach for attenuation correction in PET/CT is based on obtaining an attenuation map from the reconstructed high resolution CT images.

Metal-related artifacts might appear in the presence of high-attenuation objects (having a high atomic number) that result in an inappropriate number of photons reaching the detectors. Metallic implants such as hip prostheses, surgical clips and dental fillings induce this type of artifacts and lead to a discrepancy between reconstructed Hounsfield Units (HU) and the true attenuation coefficients. Hence the presence of metallic objects in the field of view of the CT scanner can turn out to wrong assessment of active zones in the corresponding regions.

In order to achieve a reliable attenuation map, reduction of metal artifact is inevitable. Several methods were proposed for metal artifact reduction:

1) Backward projection on a modified sinogram: since metallic objects have high gray level, a simple thresholding can be used for metal detection. The extracted image is reprojected to determine the metallic regions in the sinogram, named masked sinogram. Then, an interpolation algorithm is performed at each projection angle to fill the missing parts in metal related regions. Finally, the corrected image is reconstructed from interpolated sinogram using inverse Radon transform [1,2,3].

2) Filtering techniques: in these methods, metal artifact reduction is based on designing a suitable filter. For instance, an adaptive filtering approach is proposed by Hsieh in Radon space based on the local statistical properties of the CT projections. First the noise character-

J. Vander Sloten, P. Verdonck, M. Nyssen, J. Haueisen (Eds.): ECIFMBE 2008, IFMBE Proceedings 22, pp. 492–495, 2008

istics of a projection sample are modeled. Then a filter is designed such that its parameters are dynamically adjusted to adapt to the local noise characteristics [4].

3) Iterative reconstruction algorithms: Expectation maximization and algebraic reconstruction techniques are two common methods in this field but implementation is time consuming and might not be suitable for routine clinical application [5,6,7].

4) Hybrid methods are proposed in [8] in which a combination of the above mentioned algorithms are used.

Currently available metal artifact reduction techniques using backward projection of a modified sinogram are usually applied to raw projection data which are huge encrypted files that are not easy to decode and manipulate. Making use of a virtual sinogram produced by forward projection of CT images makes the algorithm faster and accessible. The approach proposed in this paper uses the backward projection of the corrected virtual sinogram and achieves acceptable results for metal artifact reduction in PET/CT images. It should be noted that our goal is not to generate high quality diagnostic CT image in the regions close to the artifact. Rather our MAR method is to provide artifact free μmap.

II. MATERIALS AND METHODS

A. Phantoms and scanning protocols

To investigate the effect of metal streak artifacts caused by dental fillings on the accuracy of CTAC, a jaw phantom was designed and constructed. This phantom is made of a 20 cm in diameter and 4 cm in height cylindrical plexiglass and consists of 16 syringes with different diameters filled with K_2HPO_4 solution with two different concentrations. Eight 7 mm diameter syringes and six 10 mm diameter were filled with 1800 mg/cm^3 concentration of K_2HPO_4 solution simulating teeth and two 20 mm diameter syringes were filled with 900 mg/cm^3 concentration of K_2HPO_4 solution mimicking jaw bone. These inserts were arranged in a form that is approximately similar to a real jaw. In order to generate metal artifacts in CT images, GK-110 dental amalgams were inserted in the location of posterior teeth. A clinical GE LightSpeed VCT (General Electric Healthcare Technologies, Waukesha, WI) 64 slice CT scanner was used to acquire images of the phantom. The phantom was scanned at 120 kVp and 200 mAs twice in the same position: first without any metal insertion and then with 2 metal insertions. The first scan was performed to allow assessment of the accuracy of the metal artifact correction algorithm through comparison with and without metal artifact image.

B. MAR algorithm

Most of the currently available sinogram based MAR algorithms are based on correction of raw data sinograms which are huge files usually stored in proprietary format not generally disclosed by manufacturers and thus are not straightforward to handle or manipulate. Our method uses the concept of virtual sinograms for implementation of MAR, which are produced by forward projection of CT images in 2D. This procedure was performed using a MATLAB routine. Although CT images obtained from a virtual sinogram might not be of sufficient quality for clinical diagnosis, it is suitable for the CTAC procedure. One of the reasons is that the CT images are downsampled and smoothed to match the resolution of PET images which renders them less sensitive to small inaccuracies.

In order to detect the projection data affected by metallic objects in the sinogram metallic objects are segmented by applying a simple thresholding to the original image allowing to obtain a metal-only image (fig. 1b). Thereafter this image is forward projected in 360 degrees to obtain a sinogram directly related to metallic objects. In this sinogram, the pixels with intensities greater than zero reflect the projections affected by metallic objects (fig. 1d).

The next step is to replace these projections in the original sinogram by appropriate values. To do so these affected projections are replaced by interpolated values from adjacent projections using the spline interpolation technique. Then the corrected sinogram is reconstructed in order to generate the artifact free image.

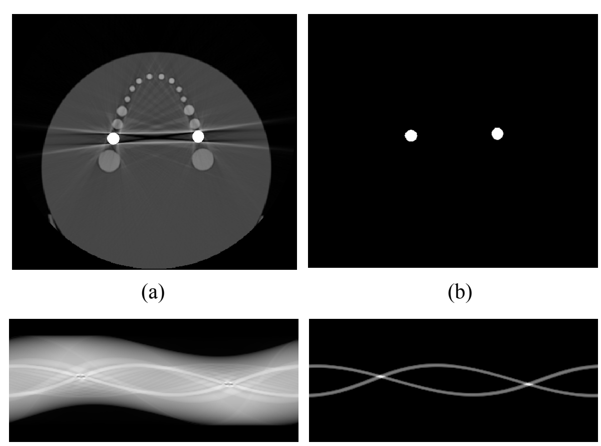

Fig. 1 Detection of affected projections: (a) original CT image, (b) metal-only image, (c) original sinogram and (d) metal-only sinogram.

To produce the μmap from the corrected CT images, three steps have to be performed. The first step is to equalize the size of the CT image and the PET image to be corrected. This is achieved by down-sampling of the corrected CT image. The second step is to match the spatial resolution of the CT and PET images. A Gaussian filter with an appropriate kernel size is applied to the CT image to achieve this goal. The linear attenuation coefficient measured with CT is calculated at the x-ray energy rather than at the 511 keV. It is therefore necessary to convert the linear attenuation coefficients obtained from the CT scan to those corresponding to the 511 keV. In this work, a bilinear calibration curve is used for energy conversion.

Likewise, the μmap without metal artifacts is produced and compared to the μmap produced by the corrected image. The comparison was performed by defining 25 regions of interest (ROIs) in different areas of the phantom including teeth, bones, areas deteriorated by artifacts and artifact-free areas. The ROI statistics were analyzed for both the corrected and artifact-free images and the results reported on Box and Whisker plots.

III. Results

The metal artifact correction algorithm was applied to the CT image of the phantom including dental filling amalgams followed by generation of the μmap (Figure 2b). Figure 2c shows the image obtained from the phantom without amalgams where no visible artifact can be observed. For comparison with the corrected μmap, regions corresponding to dental fillings were replaced with values corresponding to metal in the original image.

As can be observed in Figure 3, the ROIs were defined on jaw bones (ROIs 1 and 2), posterior teeth (ROIs 3, 4, 5 and 6), anterior teeth (ROIs 7, 8, 9, 10, 11, 12, 13 and 14), regions affected by artifact inside the teeth (ROIs 15, 16, 17, 18 and 19), regions affected by artifact outside the teeth (ROIs 20 and 21) and regions unaffected by artifact (ROIs 22, 23, 24 and 25). The same ROIs were also defined on the original μmap, corrected μmap and artifact-free μmap. Thereafter the mean values, standard deviations and standard errors of these ROIs were reported in Box and Whisker plots to illustrate the relative differences between the original μmap and the artifact-free μmap (fig. 4a) and between the corrected μmap and the artifact-free μmap (fig. 4b).

IV. Discussion

The proposed method can be used to generate attenuation maps suitable for attenuation correction of PET data thus providing a fast and convenient method allowing to correct for the presence of metal artifacts caused by dental fillings without the need to use the raw data. Its performance for eliminating artifacts in regions adjacent to metallic object is noticeable. As illustrated in Figure 4(a), metal artifacts cause an immense difference between the original μmap and the one without metal artifact in some regions including metallic object proximity and regions between two metallic objects. It can be observed from Figure 4(b) that these differences are considerably reduced using this MAR approach. It should be noted that the errors didn't change to a great extent in some regions, mostly those related to jaw bones and teeth.

The next step of this work is to apply the algorithm on clinical oral and head and neck PET/CT data, which is currently ongoing.

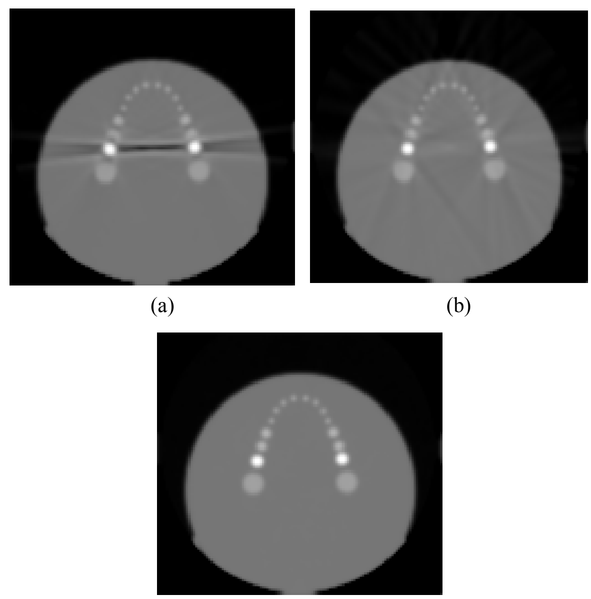

Fig. 2 (a) μmap obtained from the original image, (b) μmap obtained from the corrected image, (c) μmap obtained from without metallic artifacts.

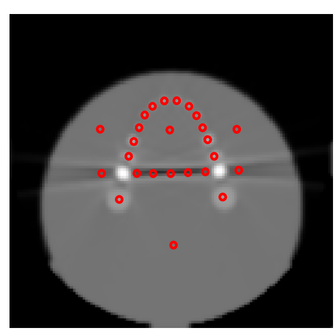

Fig. 3 ROIs defined on the μmap to evaluate the accuracy of the metal artifact correction technique.

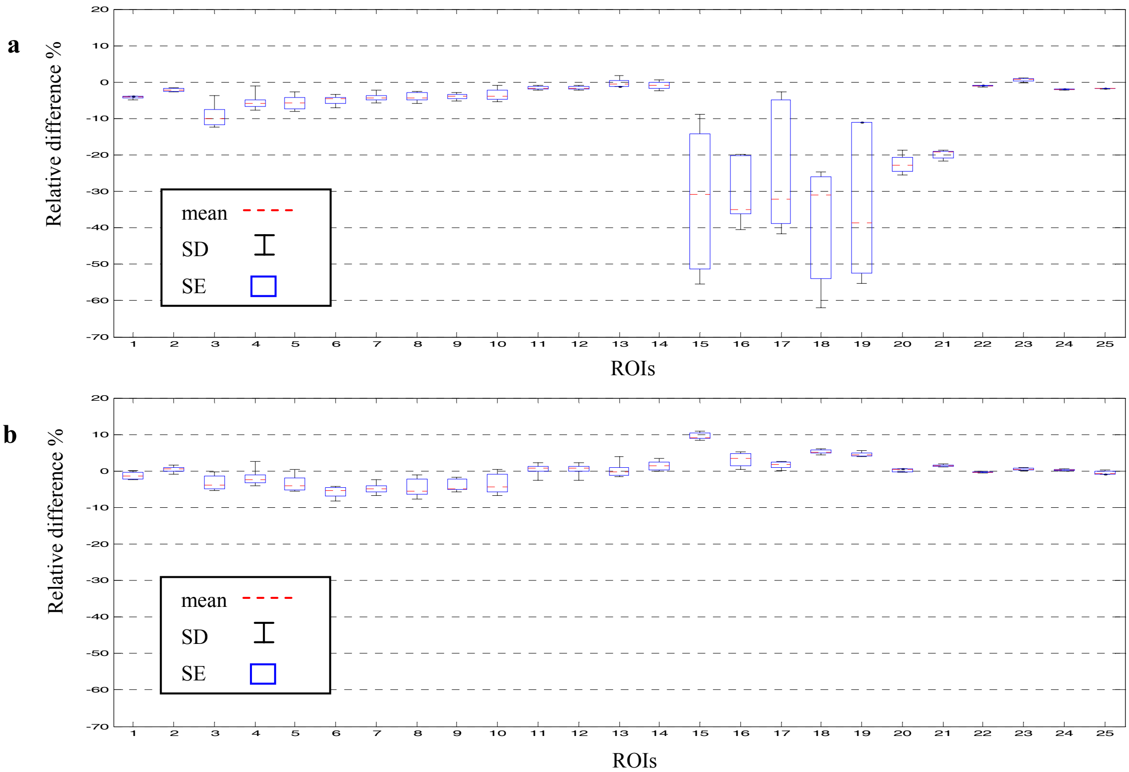

Fig. 4 Box and Whisker plots showing relative differences for 25 ROIs between a) the original μmap and without-metal μmap and b) the corrected μmap and without-metal μmap.

V. Conclusions

In this study, a fast approach was proposed for reducing dental filling artifacts on CT images used in CTAC of corrected PET data. It was concluded that the proposed method allows to reduce the strongest artifacts located in regions adjacent to metallic objects in the generated μmap, from ~35% to about 5 %.

Acknowledgment

This work was supported by Tehran University of Medical Sciences and Research Center for Science and Technology in Medicine. HZ acknowledges the support of the Swiss National Science Foundation under grant No. 3152A0-102143.

References

1. Bazalova M, Beaulieu L, Palefsky S et al. (2007) Correction of CT artifacts and its influence on Monte Carlo dose calculation. Med. Phys 34(6):2119-2132
2. Kalender W, Hebel R, Ebersberger J (1987) Reduction of CT artifacts caused by metallic implants. Radiology 164:576-577
3. Yazdi M, Beaulieu L (2006) A novel approach for reducing metal artifacts due to metalic dental implants. IEEE Nucl. Sci. Symp. Conf. Rec. 4:2260-2263
4. Hsieh J (1998) Adaptive streak artifact reduction in Computed Tomography resulting from excessive X-ray photon noise. Med. Phys 25: 2139-2147
5. Wang G, Snyder D, O'Sullivan J et al. (1996) Iterative deblurring for CT metal artifact reduction. IEEE Trans Med Imaging 15(5):657-664
6. De Man B, Nuyts J, Dupont P, et al. (2001) An iterative maximum-likelihood polychromatic algorithm for CT. IEEE Trans Med Imaging 20(10):999 – 1008
7. De Man B (2001) Iterative reconstruction for reduction of metal artifacts in Computed Tomography. PhD Thesis, University of Leuven
8. Watzke O, Kalender WA (2004) A pragmatic approach to metal artifact reduction in CT: merging of metal artifact reduced images. Eur Radiol. 14(5):849-856

† Corresponding Author: Mohammad Reza Ay
Institute: Tehran University of Medical Sciences
Street: Pour Sina
City: Tehran
Country: Iran
Email: mohammadreza_ay@tums.ac.ir